Degradation and mineralization of methylene blue using a heterogeneous photo-Fenton catalyst under visible and solar light irradiation

Journal:	*Catalysis Science & Technology*
Manuscript ID	CY-ART-09-2015-001494.R1
Article Type:	Paper
Date Submitted by the Author:	04-Nov-2015

Complete List of Authors:	Ahmed, Yunus; Universiti Kebangsaan Malaysia, Department of Chemical and Process Engineering; Chittagong University of Engineering and Technology (CUET), Department of Chemistry Yaakob, Zahira; Universiti Kebangsaan Malaysia, Department of Chemical and Process Engineering Akhtar, Parul; Universiti Kebangsaan Malaysia, Department of Chemical and Process Engineering

Degradation and mineralization of methylene blue using a heterogeneous photo-Fenton catalyst under visible and solar light irradiation

Yunus Ahmed[ab*], Zahira Yaakob[a]*, Parul Akhtar[a]

[a]*Department of Chemical and Process Engineering, Faculty of Engineering and Built Environment, Universiti Kebangsaan Malaysia, Bangi, Selangor 43600, Malaysia.*

[b]*Department of Chemistry, Chittagong University of Engineering and Technology (CUET), Chittagong-4349, Bangladesh.*

* Corresponding author.

E-mail address:

zahirayaakob65@gmail.com Tel.: +60389216420; Fax: +60389216148.

yuunusahmed@cuet.ac.bd Mobile:+880-1712637598

Abstract

The SiO_2-supported Fe and Ni bimetallic catalyst has been synthesized, characterized and, for the first time, tested as a heterogeneous photo-Fenton catalyst for the degradation and mineralization of methylene blue (MB) dye. The morphological, structural, and optical properties of this catalyst were analyzed using FESEM, XRD, FTIR and UV–vis spectroscopy. The photocatalytic degradation of MB has been investigated using Fe-Ni/SiO_2 catalysts under visible and solar light irradiation in aqueous solutions. The effects of solution pH, H_2O_2 concentration, initial MB concentration, catalyst dosage and light intensity on the degradation of MB have been systematically investigated. An almost complete degradation was achieved within 60 min with the solution pH of 3.00, H_2O_2 concentration of 3.0 mM/L and catalyst dose of 0.85 g/L. The degradation and total organic carbon (TOC) removal efficiencies were 99.80% and 86.19%,

respectively, for sunlight. However, the values were only 99.01% and 75.71% for visible light. These results suggested that Fe-Ni/SiO_2 possesses significant catalytic activity, and the solar-Fenton process is a feasible method for degrading and mineralizing the MB dye compared with artificial visible light. The catalytic action is attributed to H_2O_2 and the formation of hydroxyl radicals (•OH) by Fe (III) in Fe-Ni/SiO_2 via the photo-Fenton reactions. Furthermore, we determined that the catalyst activity can be replicated in successive experiments without a significant decline in the Fe-Ni/SiO_2 and H_2O_2 processing efficiency under light irradiation. Our results will be useful for future improvement of active heterogeneous photo-Fenton catalysts for developing organic dye-containing waste-water treatments.

Keywords:

Fe-Ni/SiO_2; Heterogeneous photo-Fenton; Sun light; Methylene blue; Degradation and mineralization

1. Introduction

Water is significant for most industries. However, colored effluents are discharged from many industries, such as textile, dyeing, leather, pharmaceuticals, paper, cosmetics, plastics and synthetic detergents. Without a proper treatment, the abovementioned industries release colored wastewaters into the environment. Color is a readily recognizable wastewater indicator and is observable at a concentration of dyes in water of as low as 1 ppm. These colored effluents contain many bio-refractory organic compounds that pose a serious risk to human health and aquatic environments[1]. It is essential to develop novel and cost-effective methods to treat these types of colored effluents.

Various treatment technologies have been used to remove organic dyes, such as biological[2], thermal, physical and chemical treatments. Certain of these techniques are not compatible with large-scale treatment due to their drawbacks. For example, biological processes are unsuitable to treat non-biodegradable wastewater and need long retention time microorganisms to degrade the contaminants. In general, aerobic and anaerobic treatment methods have been used to treat wastewater. Both processes eliminate low amounts of pollutants. Other biological processes are incompatible with wastewater treatment due to their cost-benefits or operational difficulties. Thermal methods have some limitations and expressively discharge various hazardous compounds. Physical processes may be unsuitable for wide-ranging elimination of contaminants from the system. Chemical treatments, such as flocculation[3], precipitation, coagulation[4], electrocoagulation[5], adsorption[6], and membrane technologies, require a post-treatment. Chemical flocculation and coagulation use chemicals that generate a hazardous sludge. In addition, precipitation methods have the same sludge disposal problems. Adsorption techniques have been widely used to treat dye pollutants and only require transferring the pollutants to the adsorbent, which needs to be repeatedly circulated and regenerated. Membrane technologies, such as nano-filtration, ultrafiltration, and reverse osmosis, have been used for large-scale wastewater treatment. However, these techniques have numerous operational problems and significant capital costs.

Among the chemical methods, oxidation is an efficient and appropriate method for large-scale dye wastewater treatment. Recently, advanced oxidation processes (AOPs) have received significant attention for the remediation of contaminated wastewater. This approach produces non-selective and highly reactive hydroxyl radicals (•OH) that degrade the recalcitrant contaminant present in wastewater[7-12]. The generation of •OH radical is enhanced with

conventional and non-conventional AOPs. The conventional AOPs included ozonation (O_3); a combination of ozone with UV irradiation (O_3/UV) or hydrogen peroxide (O_3/H_2O_2), or both (O_3/H_2O_2/UV); ozone combined with catalysts (O_3/catalysts); UV/H_2O_2; Fenton, Fenton-like and photo-Fenton processes (Fe^{2+}/H_2O_2, Fe^{3+}/H_2O_2 and Fe^{2+}/H_2O_2/UV), and UV irradiation, ultrasound, and (or) high electron-beam irradiation and heterogeneous photo catalysis. Conversely, the non-conventional AOPs incorporate photo-electro-Fenton and sono-electro-Fenton processes.

Recently, Fenton processes have been widely used as advanced oxidation processes (AOPs) to treat various persistent and non-biodegradable contaminants. This process has a relatively low-cost and is expected to perform well in parallel with other oxidation processes. However, the traditional homogeneous Fenton's catalysts based on ferrous or ferric salts have several disadvantages. Specifically, (i) the production of large amounts of iron sludge as a by-product after disposal[13], (ii) a narrow and low pH range (pH < 3), and (iii) deactivation of iron by iron complexing reagents such as phosphate ions[14]. To overcome these drawbacks, heterogeneous Fenton and Fenton-like catalysts have recently received significant attention. However, the iron ion concentration decreased in the heterogeneous Fenton process, and the generation of hydroxyl radicals was significantly affected by the Fe^{3+} and H_2O_2 reaction[15]. As a result, the degradation efficiency reduced. Thus, the heterogeneous photo-Fenton process is easily overwhelmed by this limitation[16]. In the presence of light, the Fe (III) ion was rapidly transformed into Fe (II) ions,[9, 17] and these ion can react with H_2O_2 to generate more hydroxyl radicals. The use of natural sunlight reduces operating costs that accompany the non-natural light source processes[18].

In addition, heterogeneous Fenton's catalyst suffers from poisoning because intermediate by-products adsorb on the surface and gradually inactivate the surface[19]. In general, bimetallic catalysts can modify the catalytic properties of one metal by another metal by changing the electronic configuration and/or surface ensemble. Consequently, both metals improve their activity, selectivity and stability[20]. In the past, the SiO_2-supported Fe and Ni loaded bimetallic catalysts have been used to decompose methane[21], to hydrogenate and decarbonylate furfural[22] and to selectively convert m-cresol[23]. Furthermore, numerous researchers have synthesized iron-enclosing meso-structured silica (i.e., Fe_2O_3/SBA-15) to oxidize phenol using sono-Fenton[24] and photo-Fenton[25]. In addition, Zhong and coworkers integrated sono–photo-Fenton to decolorize C.I. Acid Orange 7 [26], and Segura et al., (2009) used this process to degrade phenol[27]. However, Fe-Ni/SiO_2 catalysts have never been used for degrading MB under solar or visible-light irradiation in a photo-Fenton oxidation process.

The purpose of this study was to explore the photo-Fenton degradation of methylene blue dye using the Fe-Ni/SiO_2 catalyst under visible-light irradiation and to optimize and analyze the reaction conditions, such as the solution pH, H_2O_2 and MB dye concentrations, catalyst dosage and light intensity, on the degradation and mineralization of MB. In addition, comparison of a heterogeneous photo-Fenton process under solar light irradiation was performed. The results help to understand the Fe-Ni/SiO_2 catalyst photocatalytic activity.

2. Experimental

2.1. Chemicals and reagents

Methylene blue (Merck), SiO_2 (Davisil, grade 633, Sigma–Aldrich), $Ni(NO_3)_2 \cdot 6H_2O$, $Fe(NO_3)_3 \cdot 9H_2O$ and H_2SO_4 (95~98%) were purchased from R & M Chemicals, NaOH (96%) and H_2O_2 (30%, w/w) were purchased from the Aladdin industrial corporation. All chemicals were AR grade or better and used without further purification. Milli-Q water was used for solution preparation and NaOH (1.0 M) and H_2SO_4 (1.0 M) were employed for pH adjustment.

2.2. Preparation of Fe-Ni/ SiO_2 catalyst

The Fe-Ni/SiO_2 catalysts were prepared by incipient wetness co-impregnation and $Ni(NO_3)_2$ $6H_2O$ and $Fe(NO_3)_3$ $9H_2O$ were used as metal precursors. Before impregnation, the support materials like silica (Davisil, grade 633) was overnight dried in an oven at 120^0 C. The nitrate salt of the corresponding metals were liquefied in 800 ml of Mili Q water and then silica was gradually added under vigorous stirring to an aqueous solution of the both metal precursors, where after the excess of water is vaporized by heating at 85-90°C. Subsequently, the material was dried overnight in an oven at 105°C. The dried powder was then calcined in a muffle furnace at 400°C for 4 hours. The prepared catalyst was denoted as Fe-Ni/ SiO_2. The final loading of each metal in the sample was 10 weight percentage.

2.3. Characterization of catalyst

The amorphous structure of the catalyst was analyzed by a Bruker D_8 Focus Advance powder diffractometer with Cu Kα radiation (λ = 0.15406 nm), and the scan range (2θ) was from 10° to 80°. The morphological characteristic of the catalysts was investigated by field emission scanning electron microscope (FESEM) and performed on the Zeiss microscope model Supra

55VP at an accelerating voltage of 3 kV. Fourier transform infrared (FTIR) spectra were recorded on a Thermo Scientific NICOLET 6700 spectrometer in the region of 400-4000 cm^{-1} to explore the chemical functional groups.

2.4. Degradation of methylene blue dye using different light sources

The reaction vessel was made of a cylindrical borosilicate glass reactor (total capacity 1.5 L) with 11 cm inner diameter and 33 cm height, which was appropriate for accommodating an immersion well. A lamp was vertically placed in the middle of reactor within a double-wall cooling system. The reactor had three ports in the upper sections, which allowed pH, temperature and sample measurements to be performed. The photo-Fenton experiments were performed in a batch reactor using an artificial visible light produced with a 500 W Xenon lamp with a wavelength range of 300 to 800 nm to stimulate sunlight. It was possible to achieve the required light intensity by changing the optical intensity. The visible-light intensity was 115.5 mW/cm^2 and was measured using a solar power meter (Model: TES 1333, Taiwan). The reactor temperature was maintained at 29 ± 2 °C by circulating cool water using a BÜCHI Distillation Chiller B-741. Air bubbles were supplied to the photo reactor, and the mixture was stirred using a magnetic bar with a speed of 500 RPM. The photo-Fenton activity was studied by changing the parameters. Specifically, the H_2O_2 concentration was adjusted between 0.5 and 10 mM; the concentration of MB dye was between 10 and 30 mg/L, the catalyst loading was between 0.25 and 1.5 g/L, the pH range was between 1.5 and 11, and the visible-light intensity was between 43.4 and 176.4 mW/cm^2.

The reactions were performed by adding a desired amount of H_2O_2 to a pH-adjusted solution that contained catalysts and 1.2-liters of different concentrations of MB. In addition, the

initial solution pH was adjusted using 1.0 M H_2SO_4 or 1.0 M NaOH solutions. At the beginning, the catalyst was added to MB solutions that were magnetically stirred, and air was bubbled in dark conditions for 10 min to achieve the adsorption/desorption equilibrium between the contaminant and photo-catalyst prior to H_2O_2 addition. During irradiation, 5 ml samples were withdrawn at pre-set time intervals and were filtered using a 0.45 μm nylon syringe filter, and their absorbance was determined using a UV–visible spectrophotometer.

The solar-Fenton degradation experiments were performed under clear skies on sunny days. Specifically, 1 L solution in a borosilicate glass beaker was magnetic stirrer, and air was bubbled in. The experiments were performed at the Living lab and Future energy crops lab in Kuala Pilah, Negeri Sembilan, Malaysia (2° 75' N; 102° 30' E) in June of 2015 with a reaction time from 11:00 am to 12:30 pm. The solar radiation intensity was measured to be approximately 115.5-116.5 mW/cm^2 with clear skies on sunny days.

2.5. Analytical measurement

Analytical measurement of MB dye concentration: The UV–Vis spectra of MB solutions were recorded by a 756 PC UV–Vis spectrophotometer (Shanghai Yuefeng Instruments & Meters Co., Ltd.) from 200 to 800 nm. The concentrations of MB in the solution were calculated by determining the absorbance at 665 nm at predetermined time intervals from a standard curve, which was generated by using known concentrations of MB. The MB conversion was calculated by using the following equation:

$$\text{Degradation efficiency of MB } (\%) = \frac{(C0 - Ct)}{C0} * 100\ \%$$

Where C_0 is the initial concentration of MB, C_t is the resulting concentration of MB solution after treated for time t (min).

Total organic carbon (TOC) analysis: Total organic carbon (TOC) was determined to know the amount of carbon found in methylene blue dye that was degraded to CO_2 during oxidation. The mineralization efficiency was calculated by estimating the total organic carbon (TOC) using DR 2500 spectrophotometer (HACH Co., USA) followed by method 10129 after 1 hour mineralization. All the tested were repeated three times.

Metal ion analysis: The stability and reusability of the catalyst was evaluated by determining the leaching of metal ions (Fe and Ni). The metal ions were measured by using PerkinElmer Atomic Absorption Spectrophotometer (AAS) model: AAnalyst 800. Each sample measured three times.

3. Results and discussion

3.1. Catalyst characterization

The morphology of catalysts was recorded using an FESEM, and images are presented in Fig. **1**. The support silica appears as a micro flake as shown in Fig. **2** (a-b). The smooth surface was fully shielded with the accumulated metal oxide after loading both metal precursors. The size of the particles was determined to vary significantly, and the average length and width of the particles was in the range of 50–60 μm and 40–50 μm, respectively. Different magnifications of Fe- and Ni-loaded catalysts are shown in Fig. **2** (c-f). From these images, we observed that the catalyst surface was surrounded by NiO and $NiFe_2O_4$ particles, which were approximately spherical and formed aggregates. Fig. **2** (c-d) and (e-f) shows the FESEM image of the catalyst before and after the treatment.

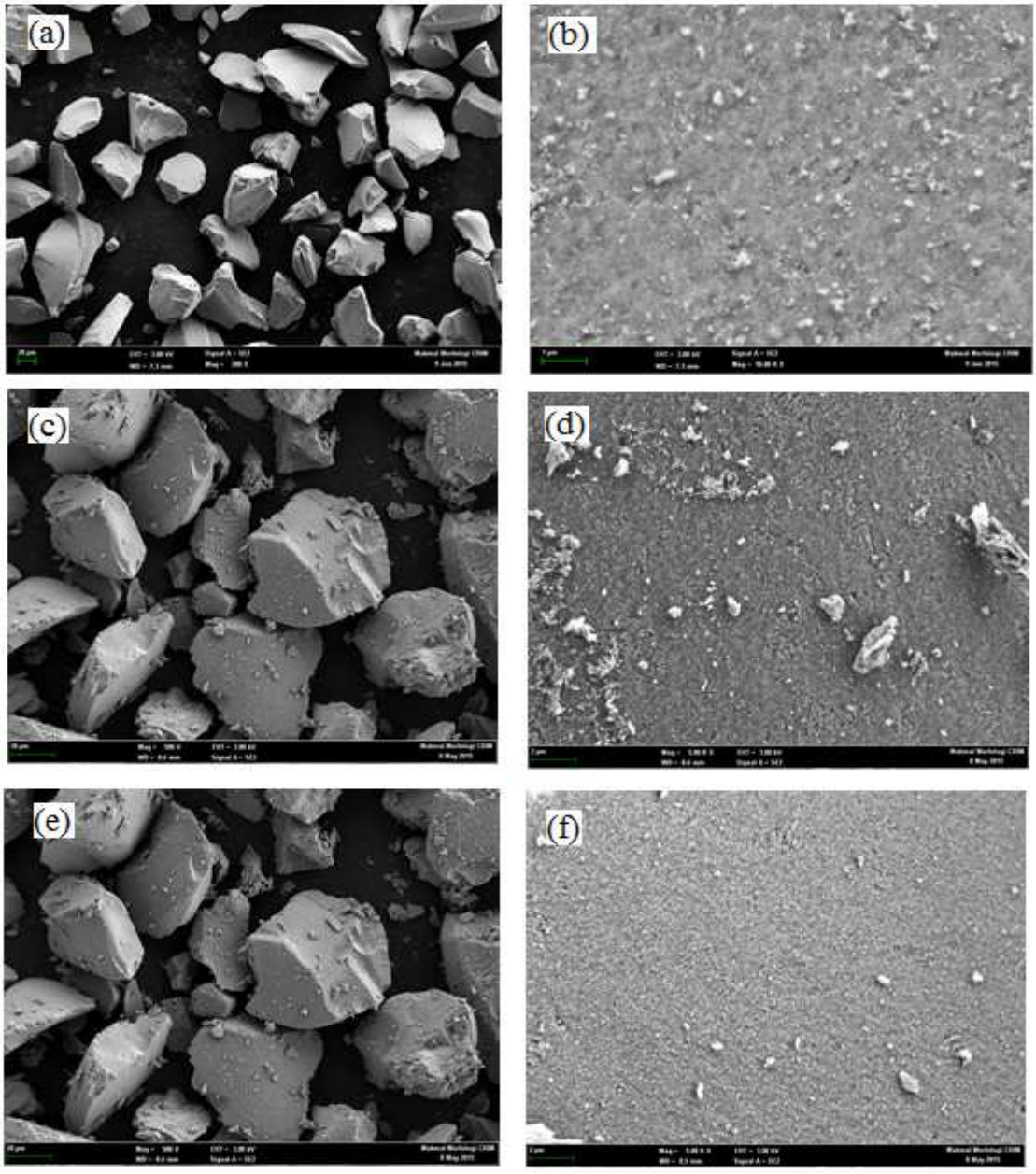

Fig. 1: FESEM images of the (a-b) support SiO_2 and (c-d) fresh Fe-Ni/SiO_2 catalysts (e-f) spent Fe-Ni/SiO_2 catalysts at different magnifications.

The X-ray diffraction pattern of Fe-Ni/SiO_2 is presented in Figure **2**. We observed wide diffraction peaks at 22° for silica (Fig. **2 a**) and a less intense diffraction hump for the metal-containing catalyst (Fig. **2 b-d**), which was attributed to NiO and Fe_2O_3. We cannot disregard the

formation of nickel ferrites ($NiFe_2O_4$) because both Fe_2O_3 and $NiFe_2O_4$ display similar diffraction patterns[28]. We also confirmed the formation of $NiFe_2O_4$ as compared to the published XRD data by Liu et al., (2013) for the synthesized of GO-doped $NiFe_2O_4$[29]. Sitthisa and coworkers observed that the Ni-loaded SiO_2 exhibited a peak at $2\theta = 44.41^o$, and both Fe- and Ni-loaded SiO_2 displayed a distinct peak in this region, which was slightly shifted to lower angles with the Fe content increase [22, 23]. Based on the above report, we can confirm the formation of $NiFe_2O_4$ on the support SiO_2.

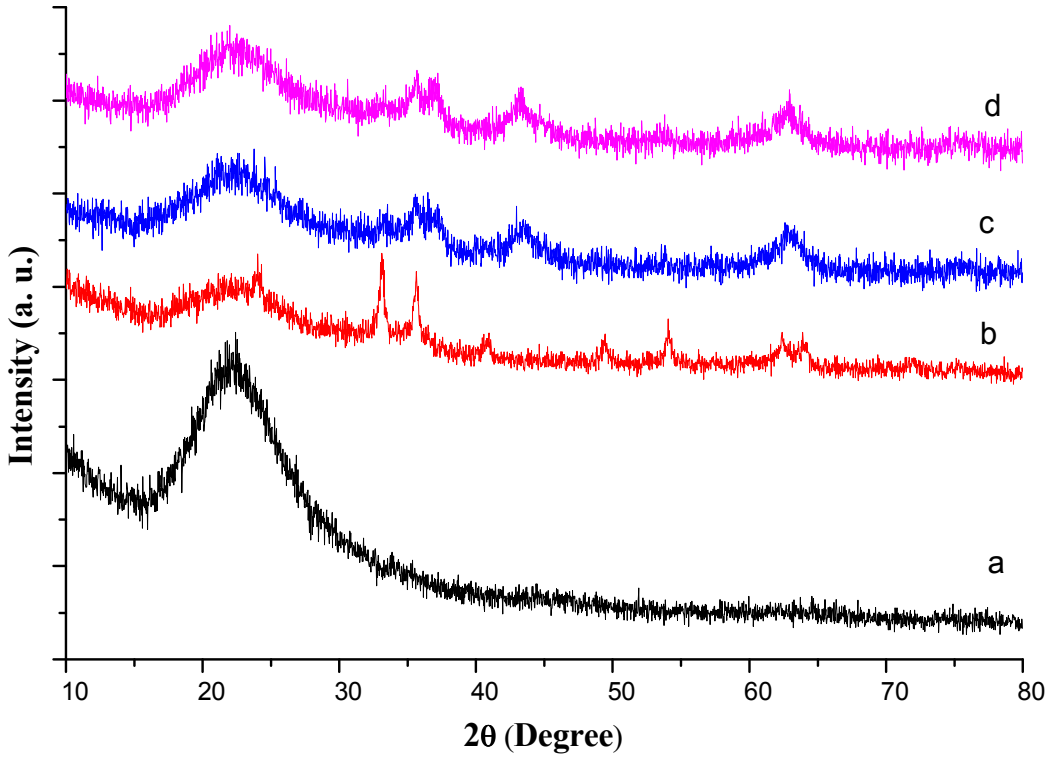

Fig. 2: XRD patterns of support and catalyst precursors. (a) SiO_2, (b) Fe/SiO_2, (c) Fresh $Fe-Ni/SiO_2$, and d) spent $Fe-Ni/SiO_2$

3.2. Catalytic activity of Fe-Ni/ SiO_2

The decolorization efficiency of the methylene blue (MB) dye was compared with the support SiO_2 only, H_2O_2 only, Fe-Ni/ SiO_2 catalyst only, visible light only, Vis./H_2O_2, Fe-Ni/ SiO_2 in

darkness, Vis./ H_2O_2/ Fe^{3+} (homogeneous Fenton), Vis./ H_2O_2/ Ni^{2+} (homogeneous Fenton), Fe-Ni/ SiO_2 with H_2O_2 in darkness (heterogeneous Fenton) and Vis./H_2O_2/ Fe-Ni/ SiO_2 (heterogeneous photo-Fenton) and the outcomes were presented in Figs. **3** and **4**. In the absence of H_2O_2 and catalyst, we achieved only 0.40% of MB decolorization efficiency after one-hour reaction with visible-light irradiation, this result indicated that the photolysis degradation was very weak and negligible. While simply 8.33 % decolorization efficiency was observed with a catalyst (Fe-Ni/SiO_2) in the dark condition. The visible light and H_2O_2 process was also to accomplish outstanding color removal efficiency. In presence of Fe-Ni/ SiO_2 catalyst and H_2O_2 in darkness, decolorization efficiency after one hour was 69.66 %, which showed that the Fe-Ni/ SiO_2 catalyst presented a good catalytic activity and could respond with H_2O_2 to produce •OH radicals to degrade the MB dye molecules. At the same time, homogeneous Ni (II) shows very lower degradation efficiency than the Fe (III) and 75.16 % of color removal efficiency achieved by this homogeneous Fe (III) catalyst.

The mechanism of the Fenton and photo-Fenton processes can be demonstrated with equations (**1**), (**2**), (**3**), (**4**) (**5**) and (**6**). The Fenton reaction accrues ferric ions (Fe^{3+}) in the system, and it does not proceed after all of the ferrous ions (Fe^{2+}) are used. Regeneration of Fe^{2+} via the photo-reduction (Eq. (**7**)) of Fe^{3+} occurs in the photo-Fenton reaction,[30] and the newly generated Fe^{2+} reacts with H_2O_2 to produce hydroxyl radicals and Fe^{3+}. Next, the cycle continues. Finally, the hydroxyl radicals (•HO) attack the MB dye, resulting in reaction intermediates that are colorless[9, 31].

$$Fe^{III}sites + H_2O_2 \rightarrow Fe^{III}sites\ H_2O_2 \quad (1)$$

$$Fe^{III}sites\ H_2O_2 \rightarrow Fe^{II}sites + {\bullet}HO_2 + H^+ \quad (2)$$

$$Fe^{III}sites + {\bullet}HO_2 \rightarrow Fe^{II}sites + O_2 + H^+ \quad (3)$$

$$Fe^{II}sites + H_2O_2 \rightarrow Fe^{III}sites + \bullet OH + OH^- \quad 4$$

$$H_2O_2 + h\nu \rightarrow 2\bullet OH \quad 5$$

$$\text{MB dye} + \bullet OH \rightarrow H_2O + CO_2 + \text{mineralization products} \quad 6$$

Fe (II) was also generated from $Fe(OH)^{2+}$ via an alternative method in the presence of light to improve the conversion between Fe^{3+} and Fe^{2+} ions and to stimulate the generation of hydroxyl radicals (•HO)[32].

$$Fe(OH)^{2+} + h\nu \rightarrow Fe^{II}sites + \bullet OH \quad 7$$

$$\text{or} \quad Fe^{3+} + H_2O + h\nu \rightarrow Fe^{2+} + \bullet OH + H^+ \quad 8$$

When the reaction was performed in solar or visible light with the Fe-Ni/SiO_2 and H_2O_2 system, the best color removal efficiency (99.80 and 99.01%, respectively) was achieved. The results demonstrated that the decolorization efficiency can be enhanced using natural sunlight or artificial visible-light radiation.

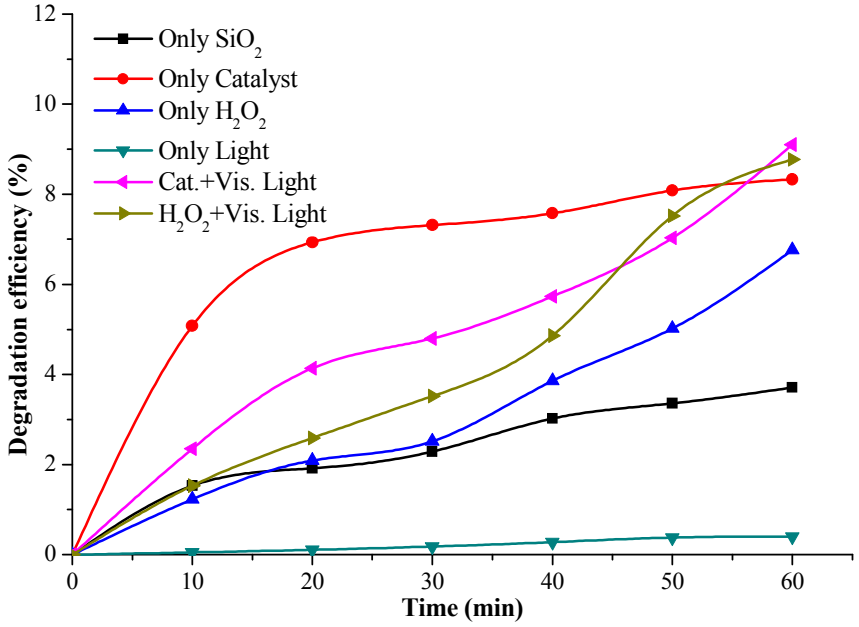

Fig. 3: Degradation efficiency of MB during 60 min under different conditions.

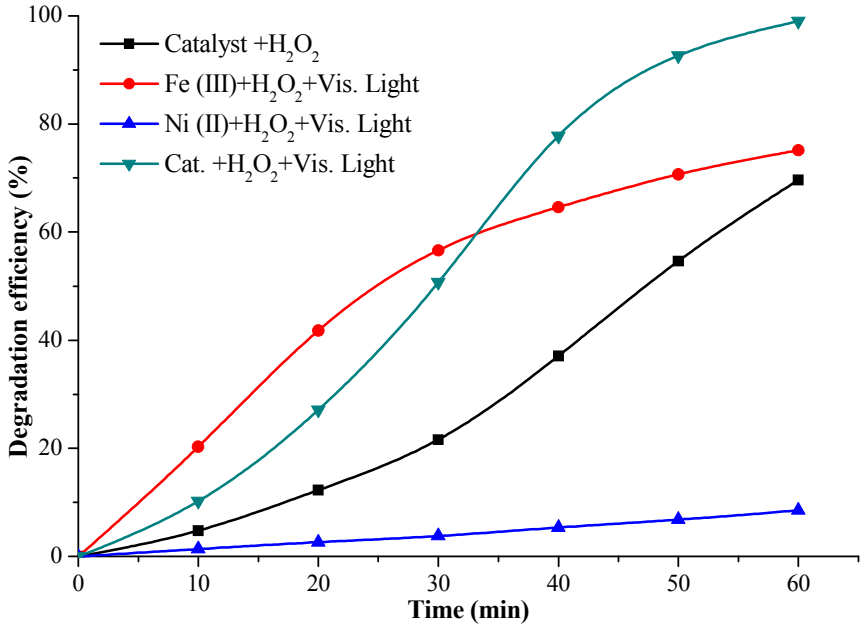

Fig. 4: Degradation efficiency of MB during 60 min under homogeneous and heterogeneous conditions.

3.3. Artificial photo degradation of methylene blue (MB) dye

3.3.1. Effect of pH on the MB dye degradation: The degradation efficiency of MB was observed at five different pH ranges of 1.50, 2.50, 3.00, 9.00 and 11.00 with a H_2O_2 concentration of 3.0 mM/L, a catalyst dosage of 0.85 g/L, a MB concentration of 20 mg/L, a visible-light intensity of 115.5 mW/cm^2, and the results are shown in Fig. **5**. We observed that the solution pH has a critical impact on the degradation of MB because of its role in controlling the catalytic action, resulting in iron ions and the stability of H_2O_2[33]. The optimum pH was found to be 3.00 in which the reaction rate was the fastest, and the maximum conversion (99.01%) was achieved within one hour. Furthermore, when the initial pH of the MB solution was extremely acidic (pH = 1.5) or alkaline (pH = 11), the degradation efficiency of MB was very low. The silica surfaces were

negatively charged in solution due to the formation of a silicic surface via the dissociation of silanol groups at the interface[34]; thus, the cationic MB dye molecule was able to absorb on the surface of the Fe-Ni/SiO_2 via electrostatic attractions.

When the initial pH decreased from 2.5 to 1.5, its degradation also decreased from 97.72% to 57.29%. The decrease in MB degradation was observed for the generation of $(Fe(II)\ (H_2O))^{2+}$, which generated less reactive hydroxyl radicals (•OH)[35]. Moreover, a scavenging effect of •OH occurred (Eq. (**9**)),[36] and hydrogen peroxide formed stable oxonium ions $[H_3O_2]^+$ (Eq. (**10**)) at lower pH. This ion also produced hydrogen peroxide that is more stable and inhibited its activity with ferric ions (Fe^{3+})[37].

$$\bullet OH + H^+ + e^- \rightarrow H_2O \qquad 9$$

$$H_2O_2 + H^+ \rightarrow [H_3O_2]^+ \qquad 10$$

However, the degradation efficiency of MB considerably reduced to 70.11% at pH=11.0, which was caused by three reasons. Firstly, the activity of Fenton reagent was reduced at higher pH, due to the sharp decrease of reaction rate, probably can be attributed to the formation of relatively inactive ferryl ion (FeO^{2+}) (Eq. (**11**))[38]. Secondly, H_2O_2 is unstable at higher pH (alkaline solution), and its auto decomposition produces H_2O and O_2 as shown in Eq. **12**[39]. Thirdly, a high-valent iron species ($Fe^{IV=0}$) might be generated in alkaline solutions, which are less reactive than hydroxyl radicals (•HO), according to Eq.13.

$$Fe^{2+} + H_2O_2 \rightarrow FeO^{2+} + H_2O \qquad 11$$

$$2H_2O_2 \rightarrow O_2 + 2H_2O \qquad 12$$

$$Fe^{II} + H_2O_2 \rightarrow Fe^{IV=0} + H_2O \qquad 13$$

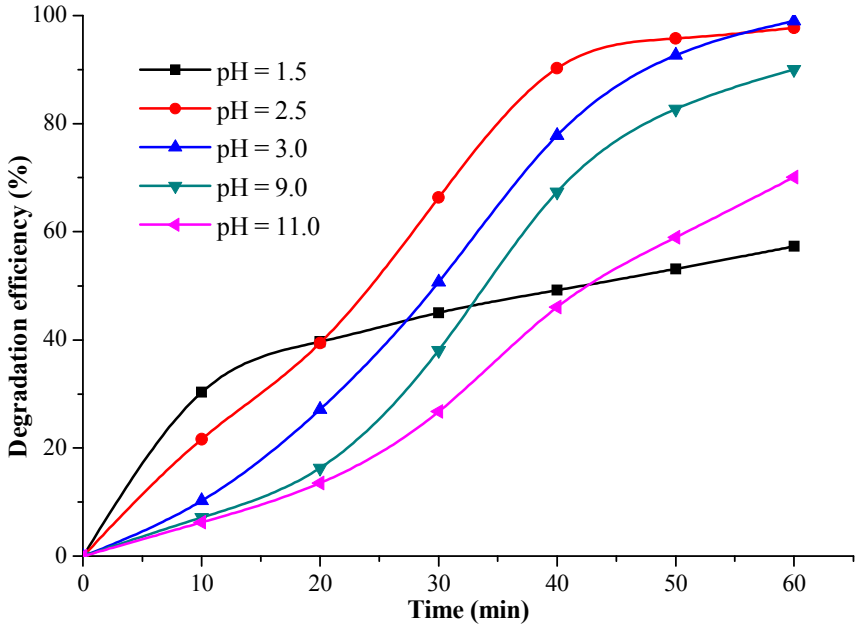

Fig. 5:. Effect of pH on the degradation of MB. Reaction conditions: an initial MB concentration of 20 mg/L, an initial H_2O_2 concentration of 3 mM/L, a catalyst load of 0.85 g/L and a visible light intensity of 115.5 mW/cm^2.

3.3.2. Effect of H_2O_2 concentration: The concentration of H_2O_2 is critical for the degradation of the MB dye during Fenton oxidation. The impact of H_2O_2 concentration on the degradation of the MB using Fe-Ni/SiO_2 is shown in Fig. **6**. The study was performed at different concentrations of H_2O_2 with a catalyst loading of 0.85 g/L, a pH of 3.00, and a MB concentration of 20 mg/L. The concentration of H_2O_2 was varied from 0.5 mM/L to 10.0 mM/L. The results demonstrate that the degradation efficiency increased with an increase in H_2O_2 concentration. When the H_2O_2 concentration was 0.5, 1.5, 3.0, 5.0 and 10 mM, the degradation efficiencies of MB were 85.39, 93.01, 99.01, 97.70 and 96.39%, respectively, at a reaction time of 60 minutes. When the concentration of H_2O_2 was in the range of 3.0 mM, almost complete (99.01%) dye removal efficiency was achieved. However, the dye removal efficiency gradually reduced as the H_2O_2

concentration increased to more than 3.0 mM. At low concentration, H_2O_2 produces less hydroxyl radicals (•HO), which slows down the rate of oxidation and degradation efficiency. H_2O_2 decomposed on the catalyst surface and produced hydroxyl (•HO) radicals. The increase in the H_2O_2 concentration from 0.5 to 3.0 mM significantly increased the reaction rate and degradation efficiency. However, the rate of degradation increased irrelevantly when the H_2O_2 concentration increased from 5 to 10 mM because of the generation of hydroperoxyl radicals ($•HO_2$), which act as scavengers of hydroxyl radicals (Eq. (**14**)). The hydroperoxyl radicals exhibited much lower oxidation capabilities and did not contribute to the MB degradation (Eq. (**15**)), which resulted in a decrease in the degradation efficiency[40]. Therefore, the further increase of H_2O_2 over its optimum level would decrease the process degradation efficiency.

$$H_2O_2 + •OH \rightarrow [H_2O] + •OOH \quad 14$$

$$•OOH + •OH \rightarrow [H_2O] + O_2 \quad 15$$

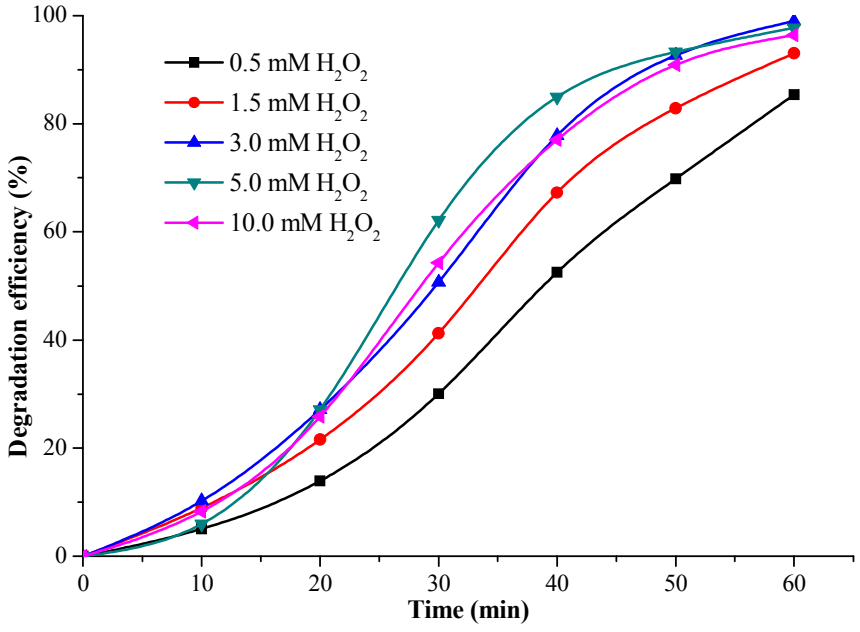

Fig. 6: Effect of H_2O_2 concentration on the degradation of MB. Reaction conditions: an initial MB concentration of 20 mg/L, a pH of 3.00, a catalyst load of 0.85 g/L and a visible light intensity of 115.5 mW/cm^2.

3.3.3. Effect of the initial MB concentration: The degradation efficiency of MB was studied by changing the concentration of the MB dye with a pH of 3.00, a H_2O_2 concentration of 3.0 mM/L, a catalyst concentration of 0.85 g/L and a visible-light intensity of 115.5 mW/cm^2, as shown in Fig. **7**. We observed that the rate of degradation increased with time at diverse initial concentrations. The decolorization efficiency increased quickly and became 99.90%, 99.50%, 99.01%, 98.23% and 94.89% at the initial MB concentrations of 10, 15, 20, 25 and 30 mg L^{-1}, respectively, after one hour of reaction. The rate of degradation increased with increasing concentration of dye molecules from 10 to 20 mg/L. However, a negative degradation efficiency was observed for the increase in dye concentration from 25 to 30 mg/L[9, 33]. This activity may be due to more MB molecules, which may be adsorbed on the catalyst surface and occupy the active sites of the catalyst when the initial concentration of the MB dye was increased. This resulted in fewer hydroxyl radicals at the surface of the catalyst[38, 41]. Thus, the reaction between H_2O_2 and the catalyst was suppressed, which decreased the rate of MB degradation. Therefore, the oxidation process required more catalyst and a longer reaction time for higher MB dye concentrations. Additionally, the molar ratio of oxidant/MB was higher for the lower MB concentrated solution because the oxidant concentration was the same for different concentrations of MB dye. A higher oxidant/MB molar ratio was favorable for MB conversions of MB[33].

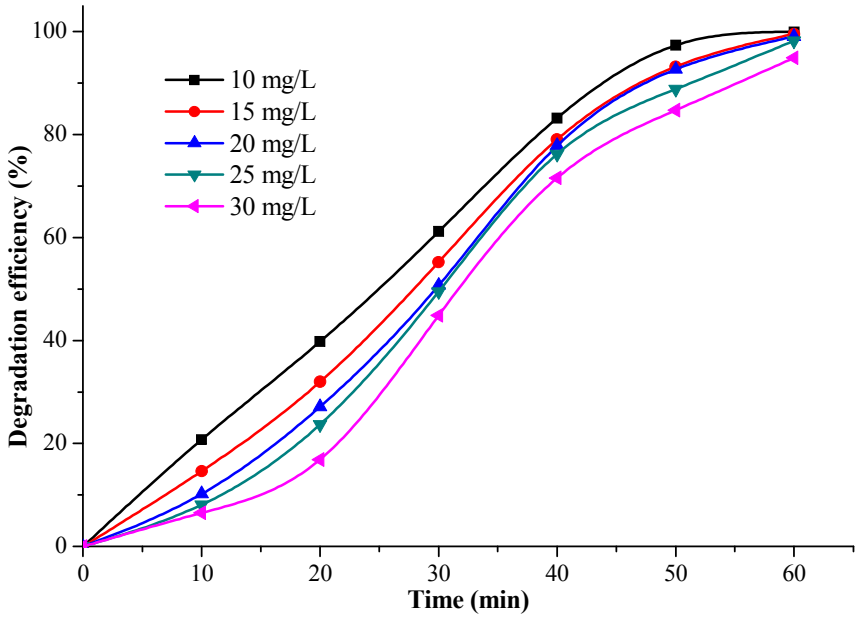

Fig. 7: Effect of dye concentration on the degradation of MB. Reaction conditions: an initial H_2O_2 concentration of 3 mM/L, a pH of 3.00, a catalyst load of 0.85 g/L and a visible light intensity of 115.5 mW/cm^2.

3.3.4. Effect of catalyst dosage: The effect of the loading catalyst on the degradation of MB by the Fe-Ni/SiO_2 bimetallic catalyst was investigated using the catalyst at 0.25, 0.50, 0.85, 1.0 and 1.5 g/L (Fig. **8**). The rate of decolorization of MB was significantly affected by the catalyst dosages. When the concentration of catalyst extended from 0.25 to 0.85 g/L, the decolorization efficiency of MB increased linearly and removed the color by 80.93, 92.17 and 99.01%, respectively. A higher degradation efficiency was observed as the catalyst dosages were increased, which increase the active sites on the surface of the catalyst (Eq. (**4**)) and generate free hydroxyl radicals (•OH). Nonetheless, the decolorization efficiency of MB was not enhanced when the catalyst was further increased in concentration from 1.0 to 1.5 g/L because of the scavenging effect of •OH radicals during unwanted side reactions (Eq. (**16**)). Thus, a nearly

complete degradation efficiency was achieved at the optimum catalyst dosage of 0.85 g/L for 1 hour of the photo Fenton reaction.

$$\equiv Fe^{II}sites + \bullet OH \rightarrow \equiv Fe^{III}sites + OH^{-} \quad 16$$

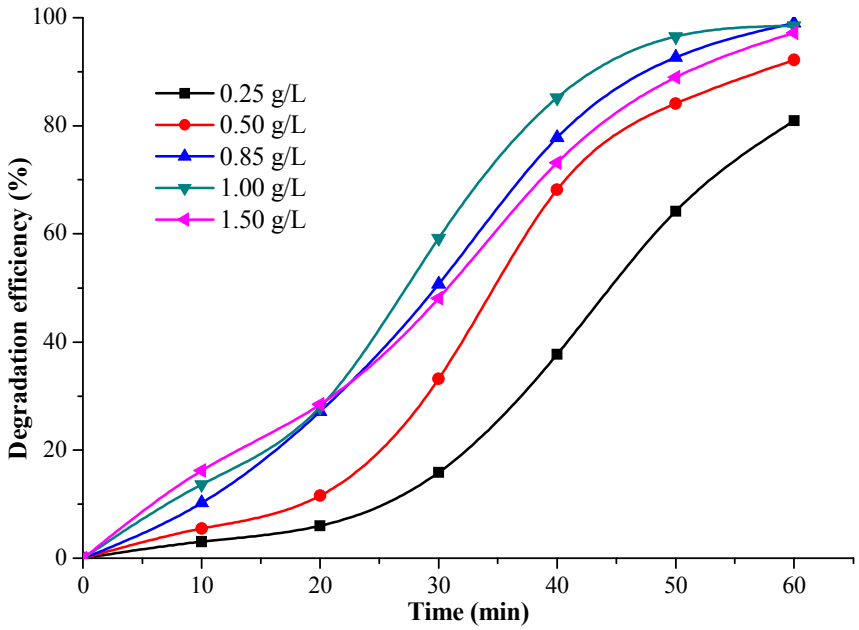

Fig. 8: Effect of catalyst dosages on the degradation of MB dye. Reaction conditions: an initial MB concentration of 20 mg/L, an initial H_2O_2 concentration of 3 mM/L, a pH of 3.00 and a visible light intensity of 115.5 mW/cm^2.

3.3.5. Effect of visible light intensity: The influence of the light intensity on the decolorization of MB was examined for Fe-Ni/SiO_2 under visible light ($\lambda > 420$ nm) and standard experimental conditions (20 mg/L of MB, 0.85 g/L of catalyst, 3 mM/L of H_2O_2 and pH =3.0), and the results are presented in Fig. **9**. The photo-degradation efficiency increased with an increase in irradiation time, illumination intensity and the wavelength of the light source. From Fig. 9, we observed that the degradation efficiency of MB increased with an increase of artificial visible-light intensity from 43.4 to 176.4 mW/cm^2. The photo-degradation rates of MB after one hour of

reaction were 82.97, 95.06, 99.01, 99.67 and 99.90% for the visible irradiation intensities of 43.4, 72.5, 115.5, 145.6 and 176.4 mW/cm^2, respectively. Generally, the photo reduction of ferric (Fe^{3+}) to ferrous (Fe^{2+}) ions (Eq. (**7**)) and the photo-generated hydroxyl radical (•OH) increased with an increase in visible-light intensity, thereby improving the color removal efficiency[42]. However, the decomposition rate of H_2O_2 under the action of ferrous (Fe^{2+}) ions is higher than for ferric ions (Fe^{3+})[43].

In the photo-Fenton process, the generation of hydroxyl radicals (•OH) primarily occurs via three mechanism: the oxidation of ferrous (Fe^{2+}) ions (Eq. (**4**)), the photolysis of H_2O_2 (Eq. (**5**)) and the photo-reduction of ferric ions (Fe^{3+}) (Eq. (**8**)). Moreover, the photolysis reaction of ferric ions (Fe^{3+}) in the presence of H_2O_2 forms Fe(III)-peroxy complexes, which may also attack the dye molecule and increase the degradation efficiency, as in Eqs. (**17**) and (**18**)[44].

$$Dye^* + Fe^{3+} \rightarrow Fe^{2+} + Dye^+ \qquad 17$$

$$Dye^+ \text{ (or dye)} + \bullet HO \rightarrow \text{Degradation Products} \qquad 18$$

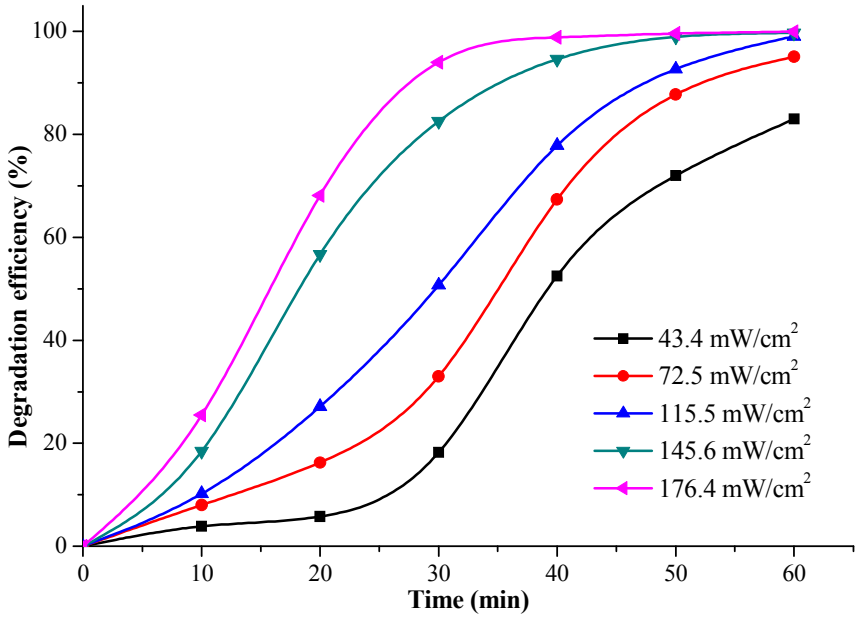

Fig. 9: Effect of visible light intensity on the degradation of MB. Reaction conditions: an initial MB concentration of 20 mg/L, an initial H_2O_2 concentration of 3 mM/L, a pH of 3.00 and a catalyst load of 0.85 g/L.

3.4. Solar photo degradation of the MB dye

3.4.1. Effect of natural sunlight irradiation: The effect of sunlight irradiation on the degradation of the MB dye was examined using the same visible-light irradiation parameters, i.e., 20 mg/L of MB dye, 3 mM of H_2O_2 and 0.85 g/L of Fe-Ni/SiO_2. The dye degradation efficiency was measured on clear sky days (1165 W/m^2) during June of 2015. The degradation efficiency of MB was examined for Fe-Ni/SiO_2 under visible light (λ > 420 nm) or in the absence of light, and it was qualitatively compared with solar light, as presented in Fig. **10**.

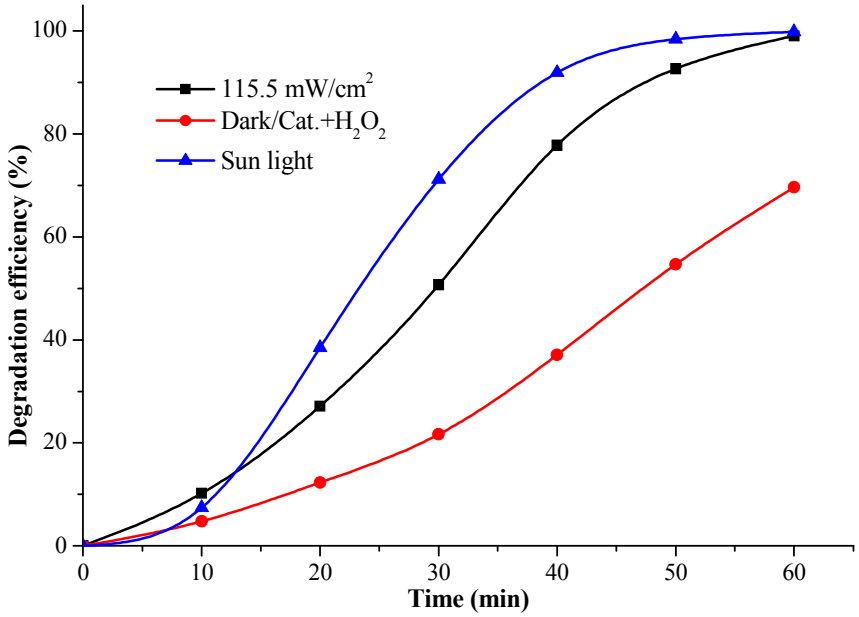

Fig. 10: Effect of light sources on the degradation of MB. Reaction conditions: an initial MB concentration of 20 mg/L, an initial H_2O_2 concentration of 3 mM/L, a pH of 3.00 and a catalyst load of 0.85 g/L.

In a control experiment, the degradation and photo-degradation of MB was examined without adding the catalyst or H_2O_2 during visible-light irradiation for one hour. We observed no significant changes in the absorption spectra and confirmed no mineralization. However, the degradation may occur under visible and solar light irradiation in the presence of Fe-Ni/SiO_2 catalyst and H_2O_2. The extent of degradation of MB under dark conditions and under visible and solar light irradiation were 69.66, 99.01% and 99.80%, respectively. In the photo-Fenton process, the photo-degradation efficiency of MB enhanced as the solar irradiation time was increased, whereas under visible light or under the dark conditions, considerably lower degradation was observed. In the solar-Fenton process, the degradation efficiencies were 71.20, 91.88, 98.38 and 99.80% for 30, 40, 50 and 60 min, respectively, whereas they were 50.72, 77.81, 92.62 and 99.01% for the visible-light Fenton process. Thus, the solar-Fenton process is more effective than the visible-Fenton process because it utilizes the ultraviolet and visible spectrum (200–800 nm). However, the visible light-assisted Fenton process (>420 nm) uses only a small amount of the ultraviolet spectrum. Therefore, the solar-Fenton reaction can produce the most photons to generate hydroxyl radicals.

The degradation of dye pollutants via the photo-Fenton process primarily depends on a few parameters such as the light intensity, reactor geometry, catalyst absorption, irradiation time and the wavelength of the light source. The intensity of the light of an artificial lamp is almost 10% less than the solar radiation at 365 nm; thus, fewer photons enter the solution and generate fewer •OH radicals. Hence, the degradation efficiency of visible light will be lower than with natural

sunlight. The reactor geometry is different for both the solar and visible lamp. In an artificial light (visible or UV) based reactor, only a limited region of the volume is efficiently illuminated during the experiments, and the required experimental time is higher than the irradiation time, whereas the irradiation time is equal to the testing time in a sunlight reaction. The slow photo-decomposition rate under visible light ($\lambda > 420$ nm) may be because the maximum absorption wavelength of the catalyst is less than 440 nm[45].

The solution depth is also an important parameter for determining the degradation rate for the photo-Fenton process[46]. In our experiments, the solution depths were 2 and 7.5 cm for visible light and solar irradiation, respectively. From Fig. **10**, we observed that the sunlight degradation rate was lower than the artificial degradation rate due to its solution depth during the first 10 minutes of the reaction. However, when the solution atmosphere meets the surrounding atmosphere under sunlight irradiation, then the degradation efficiency proportionally increased. The results suggest that the solar-Fenton process is a sensible method for the degradation of MB dye, and the use of sunlight may be a promising process for wastewater treatment, which could reduce the operating costs and be eco-friendly for the environment.

Table-1: The color and TOC removal efficiency as well as leached of metal in different light irradiation.

Light irradiation	Color			TOC			Leaching of metal	
	Initial (mg/L)	Final (mg/L)	Degradation efficiency (%)	Initial (mg/L)	Final (mg/L)	TOC removal efficiency (%)	Fe (mg/L)	Ni (mg/L)
Sun light	20	0.04	99.80	42	5.8	86.19	2.185	11.68

Visible light	20	0.199	99.01	42	10.2	75.71	1.587	11.58

3.5. Possible reaction mechanisms

According to Costa and coworkers report, the addition of nickel component in a catalyst will suppress the decomposition of H_2O_2, decreasing the oxidization activity of H_2O_2[47] but the iron atoms coordinated to oxalic acid[48] or linked to graphene[29] or utilizing higher concentration of H_2O_2 instead of oxalic acid[29] will increase the photo-Fenton activity of the heterogeneous catalyst if even nickel atoms exist in the heterogeneous catalyst. In our contrast tests, Fe-Ni loaded SiO_2 can almost degrade MB in a 3.0 mM H_2O_2 solution. In catalyst preparation both the metal nitrate react with each other and form $NiFe_2O_4$, which is adsorbed on SiO_2 support and conformed by the published report[29, 48]. In the presence of visible light irradiation, the $NiFe_2O_4$ transfer an electron from Fe3d orbital and form Fe^{2+} which sequentially reacts with oxygen in presence of H^+ ion and form H_2O_2. In case of nickel (Ni), only the Ni^{2+} species are stable and it cannot initiate the radicular reaction, which mainly exchanges Fe^{2+} in the catalyst structure[47] and form a stable and recyclable catalyst. These reactions are denoted as follows:

$$Ni^{2+}Fe^{3+}{}_2O_4 + e = Ni^{2+}Fe^{3+}Fe^{2+}O_4^- \quad 19$$

$$2\,Ni^{2+}Fe^{3+}Fe^{2+}O_4^- + O_2 + 2H^+ = Ni^{2+}Fe^{3+}{}_2O_4 + H_2O_2 \quad 20$$

$$Ni^{2+}Fe^{3+}Fe^{2+}O_4^- + H_2O_2 = Ni^{2+}Fe^{3+}{}_2O_4 + \bullet OH + OH^- \quad 21$$

In presence of light, H_2O_2 also decompose and form hydroxyl radicals (•HO)

$$H_2O_2 + h\nu \rightarrow 2\bullet OH \quad 5$$

After the formation of H_2O_2 or addition of excess of H_2O_2, it continues to react with Fe^{2+} and produces hydroxyl radicals, which can consequently react with MB dye and form the final mineralization products-

MB dye +•OH→ H_2O+ CO_2 + mineralization products 6

These mechanisms also confirmed from the above mentioned discussion. In the presence of light and Ni catalyst, only 9.1% MB degradation was achieved because Ni suppress the decomposition of H_2O_2, which confirmed the previous report by Costa et al.(2006). However, utilizing of higher amount of H_2O_2 instead of oxalic acid, almost degraded the MB dye solution, even though nickel atoms exist in the heterogeneous catalyst, which is confirmed the previous report by Liu et al., (2013).

3.6. Stability and reuse of the catalyst

The stability and reusability of the catalyst were evaluated by recycling the reactions for the degradation of MB over the Fe-Ni/SiO_2 catalyst. In each test, the catalyst was separated from its suspensions via centrifugation, then washed with an excess amount of deionized water, and then oven dried at 120°C for one hour. The catalyst retained its original red-brown color after washing and drying. The IR spectra are shown in Fig. **11**. There was no significant change between the spectra after five repeated experiments. The mineralization efficiency of MB was evaluated using the TOC reduction. The concentrations of the dye and TOC were obtained to estimate the catalyst efficiency under artificial and natural sunlight, as shown in Table **1**. The results show that the TOC removal efficiency was insignificant compared with the rate of MB dye degradation in both cases. However, a maximum TOC removal efficiency of 86.19% and 75.71% was achieved under sunlight and artificial visible light, respectively, whereas the MB removal efficiencies were 99.80% and 99.01%, respectively. Thus, the MB dyes was not completely mineralized, and the intermediate products did not display any UV−Vis peaks, as demonstrated in Figure **12a** and **12b**. The subsequent reduction of catalytic activity may have

been due to the small amounts of metal ions that leached from the surface of the catalyst. In each process, the concentration of leached iron and nickel in the solution was determined to be approximately 1.587 and 11.58 mg/L for visible light and 2.185 and 11.68 mg/L for solar light irradiation, respectively. From Table 1, we confirmed the leaching of Fe and Ni ions during both irradiations. Nevertheless, the decolorization efficiency was relatively equivalent for all the successive runs, and an approximate 97 % decolorization efficiency was attained after five runs. The results demonstrate that the catalytic behavior of the Fe-Ni/SiO_2 catalyst may be replicated in successive tests without a significant drop in process efficiency. Fig. **13** shows that the MB degradation decreases gradually during five successive runs.

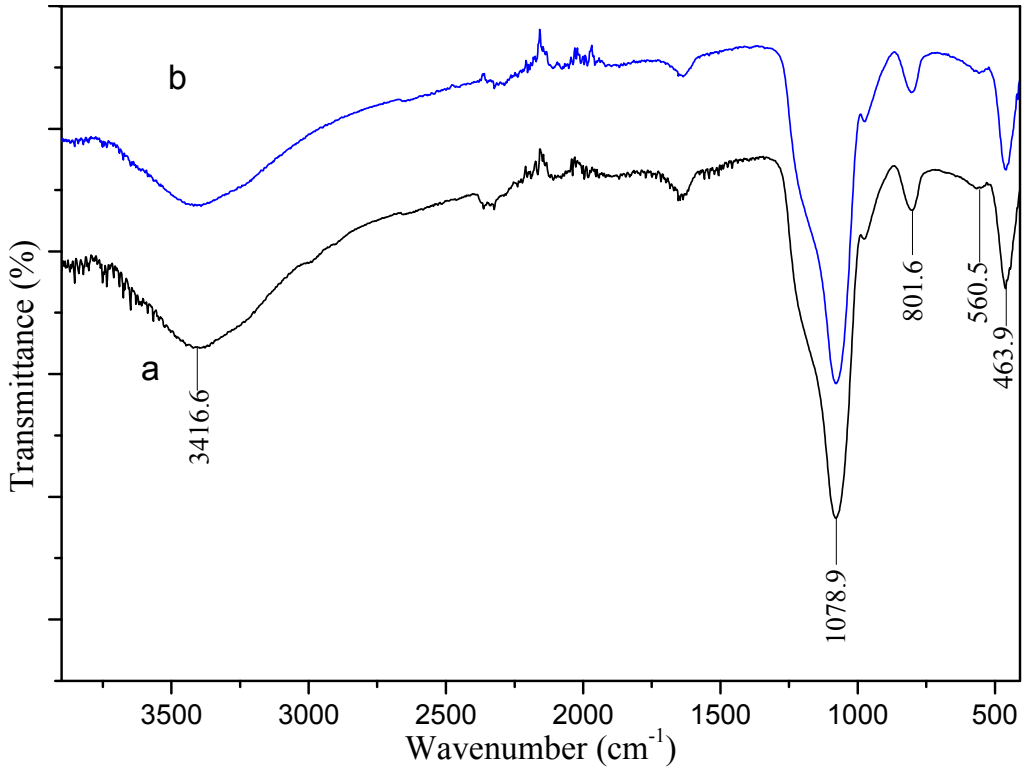

Fig. 11: FTIR spectra of Fe-Ni/SiO_2: (a) fresh and (b) after five repeated experiments

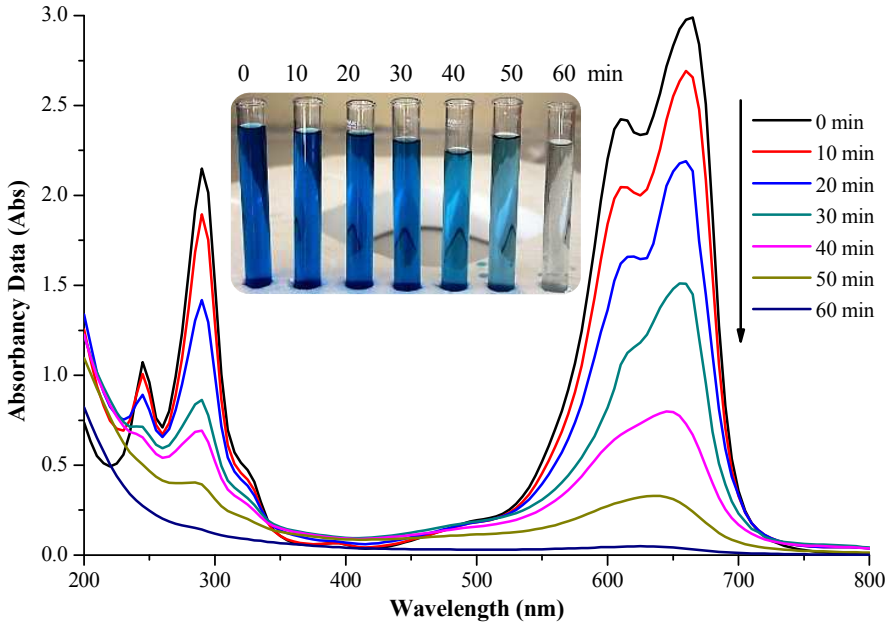

Fig. 12a: UV−Vis spectra during the visible light irradiation

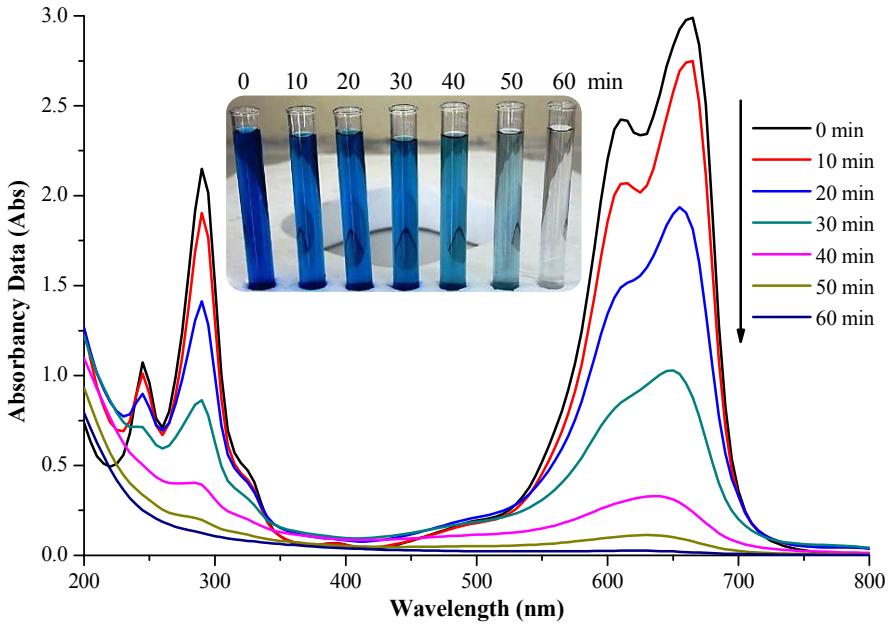

Fig. 12b: UV−Vis spectra during the sunlight irradiation

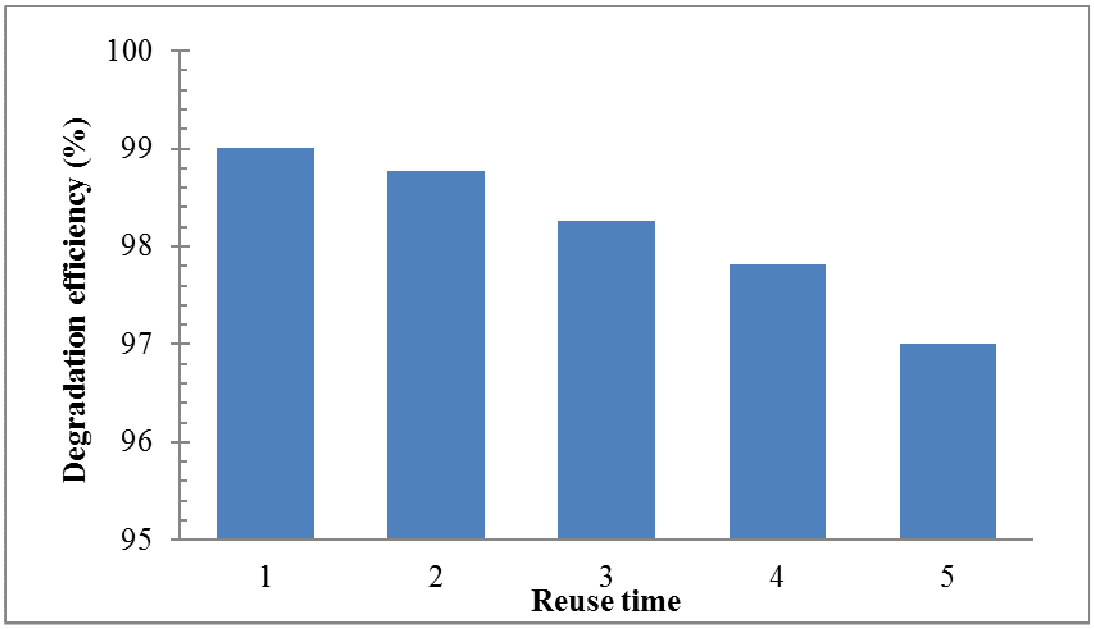

Fig. 13: Stability and reusability of the catalyst

4. Conclusions

A Fe-Ni/SiO_2 catalyst was prepared using a new wetness co-impregnation method, and this study is the first to examine the degradation of MB solutions via heterogeneous photo-Fenton catalysts. We found that they could effectively decompose the H_2O_2 into radicals. The degradation efficiency was influenced by the solution pH, concentration of H_2O_2, initial dye concentration, catalyst dosages and light irradiation. Our results suggested that the solar-Fenton process is a feasible method for the degradation and mineralization of the MB dye compared with artificial visible light, and the use of sunlight may be a promising process for reducing operating costs. The stability and reusability of the catalyst also showed that these heterogeneous photo-Fenton catalysts may overcome the shortcomings of the Fenton process. Our results may lead to future improvements of active heterogeneous photo-Fenton catalysts for the degradation and mineralization of organic dye pollutants that are similar to methylene blue.

Acknowledgments

This project is financed by the Universiti Kebangsaan Malaysia under the grants UKM-DIP-2014-011 and UKM-Simedarby KK-2014-014. The authors wish to thank the university administration for their financial support.

References

1. A. Babuponnusami and K. Muthukumar, *Journal of Environmental Chemical Engineering*, 2014, 2, 557-572.
2. G. McMullan, C. Meehan, A. Conneely, N. Kirby, T. Robinson, P. Nigam, I. Banat, R. Marchant and W. Smyth, *Appl Microbiol Biotechnol*, 2001, 56, 81-87.
3. W. Liu, H. Yuan, J. Yang and B. Li, *Bioresource Technology*, 2009, 100, 2629-2632.
4. A. K. Golder, N. Hridaya, A. N. Samanta and S. Ray, *Journal of Hazardous Materials*, 2005, 127, 134-140.
5. H. P. de Carvalho, J. Huang, M. Zhao, G. Liu, L. Dong and X. Liu, *Alexandria Engineering Journal*, 2015.
6. F. C. Wu and R. L. Tseng, *Journal of Hazardous Materials*, 2008, 152, 1256-1267.
7. J. Zhang, K.-H. Lee, L. Cui and T.-s. Jeong, *Journal of Industrial and Engineering Chemistry*, 2009, 15, 185-189.
8. M.-X. Zhu, Z. Wang and L.-Y. Zhou, *Journal of Hazardous Materials*, 2008, 150, 37-45.
9. F. Ji, C. Li, J. Zhang and L. Deng, *Journal of Hazardous Materials*, 2011b, 186, 1979-1984.
10. H. Huang, D. Y. C. Leung, P. C. W. Kwong, J. Xiong and L. Zhang, *Catalysis Today*, 2013, 201, 189-194.
11. Y. Yao, C. Zhao, M. Zhao and X. Wang, *Journal of Hazardous Materials*, 2013, 263, Part 2, 726-734.
12. P. Gayathri, R. Praveena Juliya Dorathi and K. Palanivelu, *Ultrasonics Sonochemistry*, 2010, 17, 566-571.
13. T. D. Nguyen, N. H. Phan, M. H. Do and K. T. Ngo, *Journal of Hazardous Materials*, 2011, 185, 653-661.
14. J. Deng, J. Jiang, Y. Zhang, X. Lin, C. Du and Y. Xiong, *Applied Catalysis B: Environmental*, 2008, 84, 468-473.
15. J.-H. Sun, S.-H. Shi, Y.-F. Lee and S.-P. Sun, *Chemical Engineering Journal*, 2009, 155, 680-683.
16. Y. Zhao, H. Jiangyong and H. Chen, *Journal of Photochemistry and Photobiology A: Chemistry*, 2010, 212, 94-100.
17. T. Warang, N. Patel, R. Fernandes, N. Bazzanella and A. Miotello, *Applied Catalysis B: Environmental*, 2013, 132, 204-211.
18. D. Spasiano, R. Marotta, S. Malato, P. Fernandez-Ibañez and I. Di Somma, *Applied Catalysis B: Environmental*, 2015, 170–171, 90-123.

19. D. H. Bremner, S. D. Carlo, A. G. Chakinala and G. Cravotto, *Ultrasonics Sonochemistry*, 2008, 15, 416-419.
20. M. H. Kim, J. R. Ebner, R. M. Friedman and M. A. Vannice, *Journal of Catalysis*, 2002, 208, 381-392.
21. W. Heyi, W. Wenhua, Y. Yong and P. Shuming, *J. Plasma Fusion Res. SERIES*, 2013, 10, 42-48.
22. S. Sitthisa, W. An and D. E. Resasco, *Journal of Catalysis*, 2011, 284, 90-101.
23. L. Nie, P. M. de Souza, F. B. Noronha, W. An, T. Sooknoi and D. E. Resasco, *Journal of Molecular Catalysis A: Chemical*, 2014, 388–389, 47-55.
24. R. Molina, F. Martínez, J. A. Melero, D. H. Bremner and A. G. Chakinala, *Applied Catalysis B: Environmental*, 2006, 66, 198-207.
25. F. Martínez, G. Calleja, J. A. Melero and R. Molina, *Applied Catalysis B: Environmental*, 2005, 60, 181-190.
26. X. Zhong, S. Royer, H. Zhang, Q. Huang, L. Xiang, S. Valange and J. Barrault, *Separation and Purification Technology*, 2011, 80, 163-171.
27. Y. Segura, R. Molina, F. Martínez and J. A. Melero, *Ultrasonics Sonochemistry*, 2009, 16, 417-424.
28. M. Pudukudy, Z. Yaakob and Z. S. Akmal, *Applied Surface Science*, 2015, 330, 418-430.
29. S.-Q. Liu, B. Xiao, L.-R. Feng, S.-S. Zhou, Z.-G. Chen, C.-B. Liu, F. Chen, Z.-Y. Wu, N. Xu, W.-C. Oh and Z.-D. Meng, *Carbon*, 2013, 64, 197-206.
30. B. C. Faust and J. Hoigné, *Atmospheric Environment. Part A. General Topics*, 1990, 24, 79-89.
31. W. P. Kwan and B. M. Voelker, *Environmental Science & Technology*, 2003, 37, 1150-1158.
32. D. Hermosilla, M. Cortijo and C. Huang, *Chemical Engineering Journal*, 2009, 155, 637-646.
33. Bo Yang, Zhang Tian, Li Zhang, Yaopeng Guo and S. Yan, *Journal of Water Process Engineering*, 2015, 5, 101–111.
34. E. Papirer, *Adsorption on silica surfaces*, CRC Press, 2000.
35. H. Gallard, J. de Laat and B. Legube, *New Journal of Chemistry*, 1998, 22, 263-268.
36. M. S. Lucas and J. A. Peres, *Dyes and Pigments*, 2006, 71, 236-244.
37. J. J. Pignatello, *Environmental Science & Technology*, 1992, 26, 944-951.
38. L. Xu and J. Wang, *Journal of Hazardous Materials*, 2011, 186, 256-264.
39. W. Liu, J. Qian, K. Wang, H. Xu, D. Jiang, Q. Liu, X. Yang and H. Li, *J Inorg Organomet Polym*, 2013, 23, 907-916.
40. K. Dutta, S. Mukhopadhyay, S. Bhattacharjee and B. Chaudhuri, *Journal of Hazardous Materials*, 2001, 84, 57-71.
41. M. L. Rache, A. R. García, H. R. Zea, A. M. T. Silva, L. M. Madeira and J. H. Ramírez, *Applied Catalysis B: Environmental*, 2014, 146, 192-200.
42. M. Pérez, F. Torrades, X. Domènech and J. Peral, *Water Research*, 2002, 36, 2703-2710.
43. M. Neamtu, A. Yediler, I. Siminiceanu and A. Kettrup, *Journal of Photochemistry and Photobiology A: Chemistry*, 2003, 161, 87-93.
44. Y. Xie, F. Chen, J. He, J. Zhao and H. Wang, *Journal of Photochemistry and Photobiology A: Chemistry*, 2000, 136, 235-240.
45. Y. Zuo, *Geochimica et Cosmochimica Acta*, 1995, 59, 3123-3130.
46. R. F. Pupo Nogueira, A. G. Trovó and D. F. Modé, *Chemosphere*, 2002, 48, 385-391.

47. R. C. C. Costa, M. F. F. Lelis, L. C. A. Oliveira, J. D. Fabris, J. D. Ardisson, R. R. V. A. Rios, C. N. Silva and R. M. Lago, *Journal of Hazardous Materials*, 2006, 129, 171-178.
48. S.-Q. Liu, L.-R. Feng, N. Xu, Z.-G. Chen and X.-M. Wang, *Chemical Engineering Journal*, 2012, 203, 432-439.